Journal of Alloys and Compounds 475 (2009) 9–12

Contents lists available at ScienceDirect

Journal of Alloys and Compounds

journal homepage: www.elsevier.com/locate/jallcom

Chemical solution deposition preparation of double-perovskite La_2NiMnO_6 film on $LaAlO_3$ (0 0 1) substrate

Tao Wang[a], Weibing Xu[b], Xiaodong Fang[a,*], Weiwei Dong[a], Ruhua Tao[a], Da Li[a], Yiping Zhao[a], Xuebin Zhu[c]

[a] Anhui Institute of Optics and Fine Mechanics, Chinese Academy of Sciences, Hefei 230031, PR China
[b] Jiangxi University of Science and Technology, Ganzhou 341000, PR China
[c] Key Laboratory of Materials Physics, Institute of Solid State Physics, Chinese Academy of Sciences, Hefei 230031, PR China

ARTICLE INFO

Article history:
Received 24 April 2008
Received in revised form 6 July 2008
Accepted 9 July 2008
Available online 21 August 2008

Keywords:
Thin films
Sol–gel processes
Magnetic measurements

ABSTRACT

The ordered double-perovskite La_2NiMnO_6 films were successfully deposited on $LaAlO_3$ substrate by chemical solution deposition method. Some La_2NiMnO_6 films layer with seed layer were also prepared in order to obtain higher quality films. The X-ray diffraction and Raman scattering spectroscopy are used to characterize all the films, it is found that all films are single phase with highly (0 0 l)-oriented. The field-emission scanning electron microscopy shows that the film with seed layer is relatively smooth and dense. The magnetic measurements indicate that all films exhibit a Curie temperature of about 280 K, which is close to that of the bulk material. Moreover, the low temperature magnetization of the films with and without seed layer is different, which can be attributed to that the seed layer can prevent the diffusion between the films and the substrate.

1. Introduction

Magnetic semiconductors with near room temperature ferromagnetism have attracted much attention for potential applications in spintronics devices, such as spin-based sensors, magnetic memories, magnetodielectric capacitors and spin filtering tunnel junctions [1–5]. The search for room temperature ferromagnets that are semiconducting has been extremely difficult due to conflicting requirements in the crystal structure, chemical bonding and electronic properties of semiconductors and ferromagnetic materials [1,2]. Generally, ferromagnetic semiconductors and insulators only exhibit magnetic ordering at very low temperature, such as EuS (T_C = 16 K), EuO (T_C = 77 K), $CdCr_2Se_4$ (T_C = 130 K), $EuGd_2S_4$ (T_C = 6 K), $BiMnO_3$ (T_C = 100 K), and $SeCuO_3$ (T_C = 25 K), which precludes their use in devices [3].

The ordered double-perovskite La_2NiMnO_6 (LNMO) is a ferromagnetic semiconductor, which has a curie temperature very close to room temperature (T_C = 280 K). As a result, this compound has recently attracted a great deal of attention for possible applications in spintronics devices, such as magnetodielectric capacitors and spin filtering tunnel junctions [4,5]. Large changes in the resistivity and dielectric properties have been observed in single phase bulk samples where devices could be built with commercially available solid-state thermoelectric (Peltier) coolers [4]. Aside from potential applications, the fundamental physics of this ferromagnetic semiconductor is rich and fascinating [6–8].

A bulk sample of LNMO is usually synthesized by a solid-state reaction method and crystallized in an ordered double-perovskite ($A_2BB'O_6$) structure, in which octahedral NiO_6 and MnO_6 are ordered in a rock-salt configuration [9]. Although most transition-metal oxides are antiferromagnets due to superexchange interactions between magnetic ions, LNMO is a ferromagnet. And its magnetic properties can well be explained by Kanamori–Goodenough rules. The ordered arrangement of the NiO_6 and MnO_6 octahedron gives rise to 180° ferromagnetic interactions between Ni^{2+} (d^8, S = 1) and Mn^{4+} (d^3, S = 3/2) ions [10].

Although there have been much studies on the synthesis and properties of LNMO in the bulk, there are few reports on thin films of this material. It is necessary to fabricate LNMO films for spintronics devices use. Moreover, fabrication of high-quality LNMO films will promote not only device applications but also studies of artificially layered structures with other oxides that can result in multiferroic functionality. So far, the fabrication of LNMO films is usually focused on the physical methods such as pulsed laser deposition (PLD) [11,12], and there have no relative report on the LNMO films by chemical solution deposition (CSD) method. Compared with physical methods, the chemical solution routes have some advantages such as precise control over the stoichiometry on substrate over a large area. Moreover, the CSD technology is

* Corresponding author. Tel.: +86 551 5593508; fax: +86 551 5593527.
E-mail address: twang7290@ustc.edu (X. Fang).

0925-8388/$ – see front matter © 2008 Elsevier B.V. All rights reserved.
doi:10.1016/j.jallcom.2008.07.033

simple and low-cost. Therefore, recently, the fabrication of colossal magnet-resistance (CMR) films using CSD method has attracted much attention [13,14].

In the present study, the oriented LNMO films are prepared by the CSD method on $LaAlO_3$ (LAO) (1 0 0) substrates. Some LNMO films with seed layer were fabricated in order to study its effect on the structure and properties of LNMO films.

2. Experimental procedure

LNMO films were fabricated on LAO single crystal substrates by CSD method. Lanthanum acetate, nickel acetate tetrahydrate and manganese acetate were used as raw materials. Propionic acid was used as chelating agent and butyl alcohol was used as solvent. A solution with a concentration of 0.004 M was used to prepare the seed layer and a solution with a concentration of 0.2 M was used for film deposition on LAO substrates by the CSD technique. A spin coating speed of 4000 rpm for 60 s was used in the process of depositing. The deposited films were placed on a preheated hotplate then dried at 573 K for 20 min. In order to obtain films with desired thickness, the above deposition and drying procedures were repeated for several times using the 0.2 M solutions. After that, the dried films were finally annealed at 1173 K for 2 h under the flowing O_2. For the sake of description, the films do not contain seed layer is defined as the S1; and the films contain seed layer is defined as the S2.

A Philips X'pert PRO X-ray diffractometer (XRD) and the FEI-designed Sirion 200 type field-emission scanning electronic microscopy (FE-SEM) were used to characterize the crystallization and the microstructure of the prepared films. The Raman scattering spectroscopy was measured with The LABRAMHR (France JY), with Ar^+ (514 nm) and the resolution is better than 0.5 cm^{-1}. The temperature dependence of magnetization $M(T)$ and the applied magnetic field dependence of the magnetization $M(H)$ at 5 K were measured on a quantum-designed superconducting quantum interface device (SQUID) system.

3. Results and discussion

The standard $\theta - 2\theta$ XRD patterns of the S1 and S2 are shown in Fig. 1(a). It can be observed that the diffraction peaks of the S1 belonging to LNMO phase are observed in the 2θ scanning range from 20° to 50° besides the peaks of the LAO substrates, implying that the LNMO film is single phase and has a preferential orientation with pseudocubic structure ($A_2BB'O_6$). It is similar to the film fabrication by PLD, which are advantageous for the growth of orientated films. These results can be ascribed to the less lattice mismatch between LNMO (1 0 0) films and $LaAlO_3$ (1 0 0) substrates. Additionally, there are no differences between XRD results of the two samples, which suggest that the seed layer of the S2 has no influences on the crystalline of the LNMO sample. Fig. 1(b) shows the rocking curve of the S2. It can be seen that the relatively small full width at half maximum (FWHM) of rocking curve, which also indicate that the LNMO film is (0 0 1)-oriented. However, the FWHM of the rocking curve is about 0.6°, which indicates our sample is not good epitaxy.

Fig. 2 shows the SEM results of the S1 and S2, respectively. It can be seen that the S2 is relatively dense compared with the S1, though the two films both contain some porosity, which can be attributed to the seed layer. The seed layer can prevent the diffusion between the films and the substrate, which is helpful for the LNMO film growth.

Fig. 3 shows the Raman spectroscopy of the S1 and S2. As seen from Fig. 3, there are no obvious differences in these spectra, which suggest that all the samples have essentially the same composition.

According to the recent reports on the Raman spectroscopy of the LNMO, the cubic perovskite aristotype has no Raman active vibrational modes [15,16]. Distortions from cubic symmetry occur via co-operative rotation/tilting of octahedron, displacements of the A or B cations, or B site ordering. These result in an increased unit cell and reduction in the symmetry, so the Raman active modes appear at the Brillouin zone center [16]. The number and relative intensity of peaks appeared in the Raman spectroscopy is intimately related to the degree of distortion from the ideal cubic crystal structure. For a Pnma cell, 24 modes ($7A_g + 7B_{1g} + 5B_{2g} + 5B_{3g}$) are Raman active. From Fig. 3, the spectroscopy are dominated by peaks at around 530 (A_g) and 675 cm^{-1} (B_{2g}), which are readily assigned to octahedral B–O stretching vibrations [11,16–21]. The B–O stretching peaks in our spectra are broad and asymmetric, which can be explained by the work of Bull and McMillan [16]. First, the B and B' sites are not completely ordered, and the different B–O stretching vibrations lie closely in frequency, so that unresolved contributions from different BO_6 and $B'O_6$ environments are present within the band envelope. Second, because there is a dependence of B–O stretching frequency on the oxidation state of the metal cation, the band envelope also reflects a range of local oxidation states, depending upon the environment, which will then determine the covalency of the B–O bonding. Finally, ordering of B and B' cations results in a lowering of the symmetry, and thus a change in the Raman activity of B–O stretching vibrations. Domains with differing degrees of B and B' order will result in different contributions to the B–O stretching bands.

In addition to these two modes, two high-frequency scattering features around 1209 and 1334 cm^{-1} are also observed in Fig. 3. These two peaks are quite broad and weak and appear to be related to combination and overtone modes of the fundamental stretching modes. These results are similar to the earlier report [11]. It likely accounts for the second-order two-phonon process in the ordered double-perovskite LNMO.

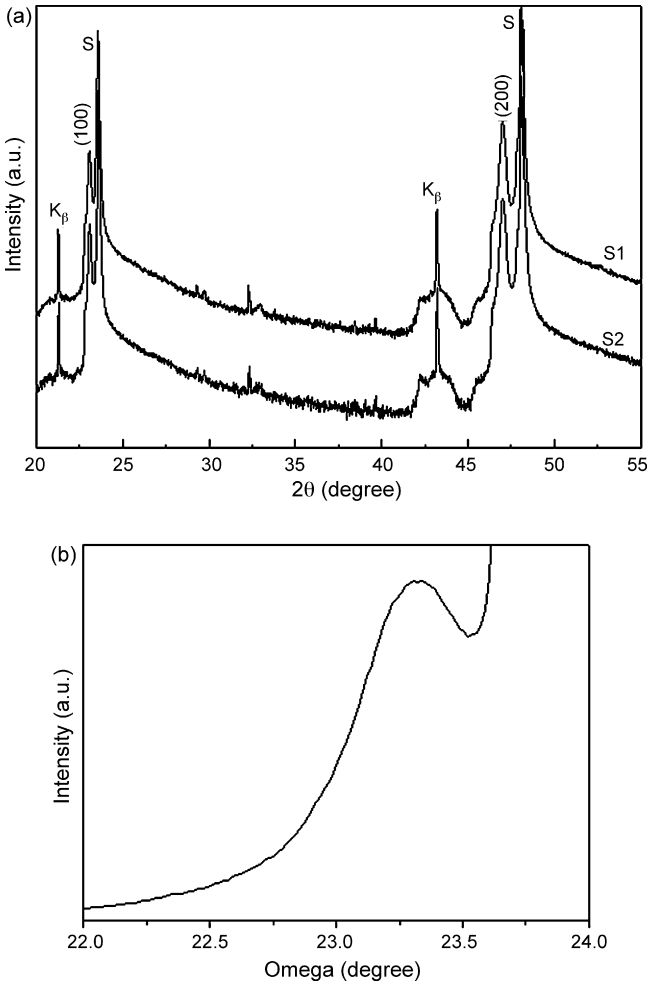

Fig. 1. The XRD results of the two LNMO samples: a (the standard XRD $\theta - 2\theta$ pattern); b (the rocking curve of the S2).

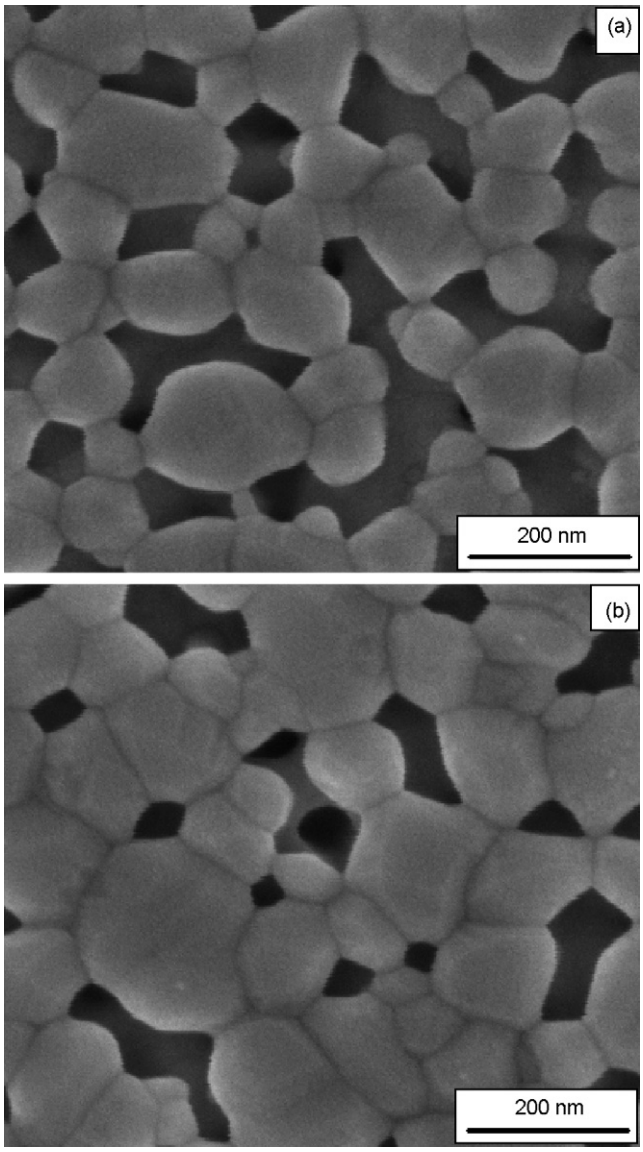

Fig. 2. The SEM results of the LNMO samples: a (S1) and b (S2).

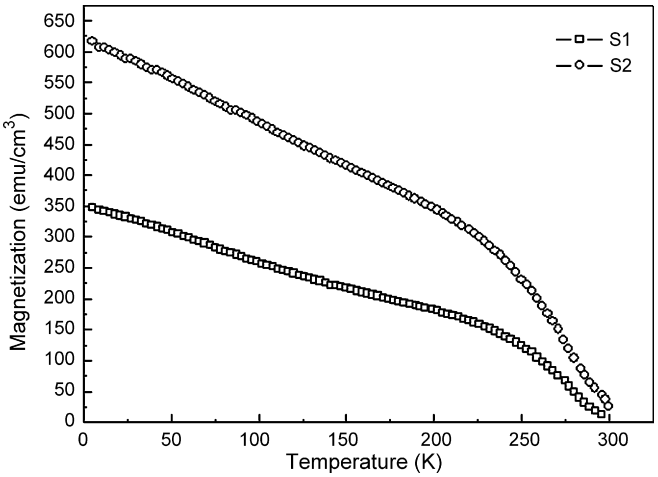

Fig. 4. The temperature dependence of the magnetization $M(T)$ obtained at an applied magnetic field of 1 T parallel to the film surface.

Fig. 4 shows the temperature dependence of the magnetization $M(T)$ obtained at an applied magnetic field of 1 T parallel to the film surface. According to the temperature dependence of the first derivative of $M(T)$, the magnetic transition temperatures (T_C) of the S1 and S2 are estimated to be 277 and 274 K, respectively. Because of the seed layer, the absolute magnetization of the S2 increased significantly, as shown in Fig. 4. However, no obvious change was observed in the onset of magnetic transition. These results imply that the films with seed layer can transport oxygen better through diffusion, enhancing the overall crystallographic order, but the seed layer does not significantly reduce the overall strain in the film—the component that was found partially responsible for the magnetic behavior in previous studies [22]. In addition, other critical parameters, such as the reduction of the dead layer at the LNMO/LAO interface due to the seed layer, may have a contributed to the two times magnetization enhancement at 5 K. However, further interface studies are necessary to confirm this. The field dependence of the magnetization at 5 K for LNMO films is shown in Fig. 5. The M vs. H plots exhibit the expected ferromagnetic hysteresis behavior for the two samples with the same coercive field about 700 Oe, which is similar to that of previous reports [11,12].

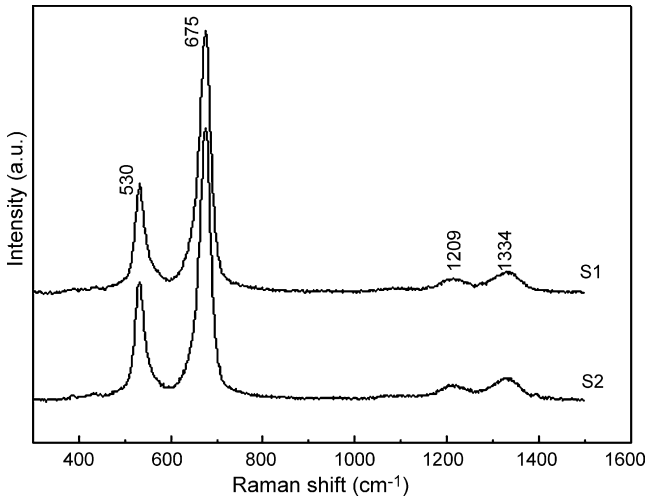

Fig. 3. The Raman spectra of the S1 and S2 at room temperature.

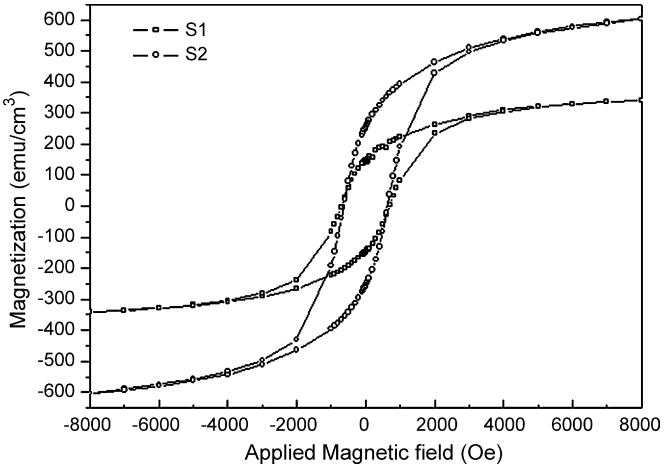

Fig. 5. The field dependence of the magnetization at 5 K for the two LNMO samples.

4. Conclusion

In summary, oriented LNMO films with an ordered double-perovskite structure have been successfully prepared using CSD method. The X-ray diffraction patterns and Raman scattering spectroscopy reveal that all films are single phase with highly (0 0 l)-oriented. The seed layer has no influence on the crystallization and the Curie temperature of the LNMO film. The Curie temperature of the LNMO films is about 280 K, which is close to that of bulk material. However, the low temperature magnetization is enhanced by the seed layer. So, further interface studies are necessary to confirm this.

Acknowledgments

Financial support from the Director's Fund of Hefei Institutes of Physical Science, Chinese Academy of Sciences and from the Chinese Academy of Sciences under the Program for Recruiting Outstanding Overseas Chinese (Hundred Talents Program) is gratefully acknowledged.

References

[1] S.A. Wolf, D.D. Awschalom, R.A. Buhrman, J.M. Daughton, S. von Molnar, M.L. Roukes, A.Y. Chtchelkanova, D.M. Treger, Science 294 (2001) 1488.
[2] D.D. Awschalom, M.E. Flatte, N. Samarth, Sci. Am. 286 (2002) 66.
[3] J. Li, Ph.D. Thesis, Oregon State University, UIM number 3169765, 2005, P. 123.
[4] N.S. Rogado, J. Li, A.W. Sleight, M.A. Subramanian, Adv. Mater. 17 (2005) 2225.
[5] H. Itoh, J. Ozeki, J. Inoue, J. Magn. Magn. Mater. 310 (2007) 1994.
[6] A. Wold, R.J. Arnott, J.B. Goodenough, J. Appl. Phys. 29 (1958) 387.
[7] J.B. Goodenough, A. Wold, R.J. Arnott, N. Menyuk, Phys. Rev. 124 (1961) 373.
[8] G. Blasse, J. Phys. Chem. Solids. 26 (1965) 1969.
[9] R.I. Dass, J.Q. Yan, J.B. Goodenough, Phys. Rev. B 68 (2003) 064415.
[10] J.B. Goodenough, Phys. Rev. 100 (1955) 564.
[11] H. Guo, J. Burgess, S. Street, A. Gupta, T.G. Calvarese, M.A. Subramanian, Appl. Phys. Lett. 89 (2006) 022509.
[12] M. Hashisaka, D. Kan, A. Masuno, M. Takano, Y. Shimakawa, T. Terashima, K. Mibu, Appl. Phys. Lett. 89 (2006) 032504.
[13] W.W. Dong, X.B. Zhu, R.H. Tao, X.D. Fang, J. Crystal Growth 290 (2006) 180.
[14] X.B. Zhu, J. Yang, B.C. Zhao, Z.G. Sheng, S.M. Liu, W.J. Lu, W.H. Song, Y.P. Sun, J. Phys. D: Appl. Phys. 37 (2004) 2347.
[15] C.L. Bull, D. Gleeson, K.S. Knight, J. Phys.: Condens. Matter. 15 (2003) 4927.
[16] C.L. Bull, P.F. McMillan, J.Solid State Chem. 177 (2004) 2323.
[17] M.N. Iliev, M.V. Abrashev, V.N. Popov, V.G. Hadjiev, Phys. Rev. B 67 (2003) 212301.
[18] L. Martín-Carrón, A. de Andrés, Eur. Phys. J. B 22 (2001) 11.
[19] M.N. Iliev, H. Guo, A. Gupta, Appl. Phys. Lett. 90 (2007) 151914.
[20] M.N. Iliev, M.V. Abrashev, A.P. Litvinchuk, V.G. Hadjiev, H. Guo, A. Gupta, Phys. Rev. B 75 (2007) 104118.
[21] H.Z. Guo, A. Gupta, M. Jiandi Zhang, S.J. Varela, Pennycook, Appl. Phys. Lett. 91 (2007) 202509.
[22] A.K. Pradhan, D. Hunter, T. Williams, B. Lasley-Hunter, R. Bah, H. Mustafa, R. Rakhimov, J. Zhang, D.J. Sellmyer, E.E. Carpenter, D.R. Sahu, J.-L. Huang, J. Appl. Phys. 103 (2008) 023914.